Intermolecular energy transfer probabilities from trajectory calculations: A new approach

V. Bernshtein and I. Oref

Citation: The Journal of Chemical Physics **108**, 3543 (1998); doi: 10.1063/1.475750
View online: http://dx.doi.org/10.1063/1.475750
View Table of Contents: http://scitation.aip.org/content/aip/journal/jcp/108/9?ver=pdfcov
Published by the AIP Publishing

Intermolecular energy transfer probabilities from trajectory calculations: A new approach

V. Bernshtein and I. Oref[a)]
Department of Chemistry, Technion-Israel Institute of Technology, Haifa 32000, Israel

(Received 23 September 1997; accepted 25 November 1997)

A new method to calculate intermolecular energy transfer probability density function $P(E',E)$ from trajectory calculations is proposed. The method distinguishes between effective trajectories that contribute to $P(E',E)$ and those with very large impact parameter which do not. The $P(E',E)$ thus found obeys conservation of probability and detailed balance and is independent of the impact parameter. The method is demonstrated for benzene–Ar collisions at various temperatures and internal energies. With this method it is possible to combine *ab initio* inter and intramolecular potentials with trajectory calculations, obtain $P(E',E)$ and use that in master equation calculations to obtain rate coefficients and populations distributions without resorting to any *a priori* assumptions and energy transfer models. In addition, the effects of internal energy, temperature and rotations on the average energy transferred are discussed. Global potentials in center-of-mass and minimal distance coordinates which are obtained by averaging 20 000 and 50 000 trajectories are reported. It is shown that Lennard-Jones or *ab initio* pairwise potentials yield a Buckingham-type global potentials. © *1998 American Institute of Physics.* [S0021-9606(98)02109-6]

I. INTRODUCTION

Collisional energy transfer, CET, plays a major role in gas phase photophysical, photochemical and thermal processes.[1] In the former, energy transfer at low and high levels of excitation provides the preferred routes of vibration to vibration–rotation–translation energy relaxation.[2] In photochemical and thermal processes, CET is part of the reactive mechanism. It provides the mechanism by which energy is pumped up and down the energy ladder.[1(b),3] Thus, collisions cool highly excited molecules and excite molecules which are located in the part of the population distribution which is far below the threshold value for reaction. The energy transfer probability function from initial energy state E to final state E', $P(E',E)$, is an elusive quantity which is extremely hard to measure[1] or calculate. Most experiments do not give the whole functional form but only the average energy transferred per collision $\langle \Delta E \rangle$ which is the first moment of the distribution.[1(a)] In the rarest of cases, the second moment can also be obtained as well. Recent physical experiments which utilize spectroscopic means give greater insight into the shape of the function. However, even in these experiments, *a priori* assumptions must be made in order to fit the data to an assumed function.[2] Knowledge of $P(E',E)$ is a prerequisite for the solutions of master equations which are used to fit experimental data and obtain population distributions and rate coefficients. The absence of known $P(E',E)$ led in the past to the development of many empirical energy transfer models which were used in master equation calculations of unimolecular rate coefficients.[1(b),4] Without such models the great progress, due mainly to Marcus and Rabinovitch and their coworkers, in understanding unimolecular reactions which was made since the late 1950's would have come to nothing. It is clear therefore that without reliable $P(E',E)$ no progress can be made in understanding the dynamics of energy transfer and reactive systems.

Lately, quasi-classical trajectory calculations have provided new insights into the collisional process.[5] The ability to selectively probe the parameters which govern the energy transfer process provide an important technique by which the principal elements which affect the energy exchange can be studied. The effects of the intermolecular potential, of the mass, internal excitation, temperature, collision duration and internal modes were studied in a systematic way. An important feature of trajectory calculations is the ability, in principle, to evaluate $P(E',E)$.[6(a),6(b)] This is done by binning the trajectories according to the value of the ΔE transferred and plotting the resultant histogram. The histogram thus obtained, is then converted into a continuous function by statistical fitting procedures. Regretfully, there is an ambiguity in this procedure. The elastic peak $(\Delta E=0)$ is unknown since it is dependent on the maximum value of the impact parameter, b_m which is chosen in the calculations with some degree of arbitrariness. This is a major obstacle which results in $P(E',E)$ not being fully determined. In the past, *a priori* assumptions were made in order to obtain the complete form of $P(E',E)$. A common approach was to use the elastic peak $(\Delta E=0)$ as the normalization constant,[6(c)] $P(E,E)\delta E = 1-\Sigma P(E',E)\delta E$. However, this is not a satisfactory solution since $\Sigma P(E',E)$ is impact parameter dependent and $P(E,E)$ can have any value depending on the value of b_m chosen in the calculations. Detailed balance was taken care of, in this method, by using only the down collisions wing of $P(E',E)$ and calculating the up-collisions wing from detailed balance. In spite of the shortcomings of the method, trajectory calculations provided in the past and still provide an important tool for understanding energy transfer. Quan-

[a)]Author to whom correspondence should be addressed.

tum and classical calculations show that there is a general agreement between the two types of calculations for benzene[5(r)] and for CS_2,[7] lending important theoretical support to studying collisional energy transfer by quasiclassical trajectory calculations. In the present work we report a new method of obtaining $P(E',E)$ from trajectory calculations which eliminates the pitfalls and shortcomings of previous approaches.

II. THEORY

A. Details of the trajectory calculations

The numerical methods used in the present work are reported in Refs. 5(n) and 5(o). The equations of motion were integrated by using a modified public domain program VENUS.[8(a)] The intermolecular potential were pairwise *ab initio*[8(b)] or Lennard-Jones potentials. The latter parameters were evaluated by the method of Ref. 5(m) and are given in Ref. 5(r). Basically, the well depth ε and the collision radius σ of the C–Ar and H–Ar L-J interactions are given by Ne–Ar and He–Ar values, respectively, calculated by the normal combination rules. The parameters are then adjusted to give the overall effective ε, σ values. The intramolecular potential includes all the normal modes contributions, stretching, bending and wagging. The values of the parameters of this potential were obtained from modified valance force field calculations by Draeger[9] and are also given in Refs. 5(n) and 5(o). The initial translational and rotational energies were chosen from the appropriate thermal energy distributions. The initial impact parameter was chosen randomly between 0 and its maximum value b_m. The initial internal energy was varied systematically. The beginning and the end of a collision were determined by the forward and backward sensing (FOBS) method.[5(n),5(o)] In this method each trajectory is scanned forward and the time is noted when, for the first time, a change ε^*, in a time period τ is observed in the internal energy of the hot molecule. Then, the trajectory is scanned backward and again, when a change ε^* is detected the time is noted again. These two times bracket the collisional event. The values of ε^* and of τ are optimized at each temperature used. They were obtained after a careful study in which ε^* and τ were changed systematically and the final values chosen such that a small variation in ε^* or in τ did not alter the initial FOBS time or duration of the collision.[5(n),5(o)] At 300 K, the value of τ was 20 fs and the value of ε^* was 70 cm^{-1}. For each trajectory the change in initial energy was noted as well as its duration as determined by FOBS.

The value of the maximum impact parameter b_m was determined separately.[5(n),5(o)] Values of 0.9 and 1.5 nm were used in the present calculations. A systematic study of post collision distances between Ar and the closest atom of the molecule has shown that for distances larger than 0.8 nm, no changes in the values of the integral of $\langle \Delta E \rangle_{\text{all}}$ were observed, therefore, this value was taken as the terminal distance for all trajectories and the end point from which the back sensing of FOBS was initiated. Convergence of $\langle \Delta E \rangle_{\text{up}}$ and $\langle \Delta E \rangle_{\text{d}}$ as a function of the number of trajectories was obtained well below the numbers of trajectories, 20 000 and 50 000, used in the present study. The large number of trajectories was chosen to provide good statistical sampling in the binning process.

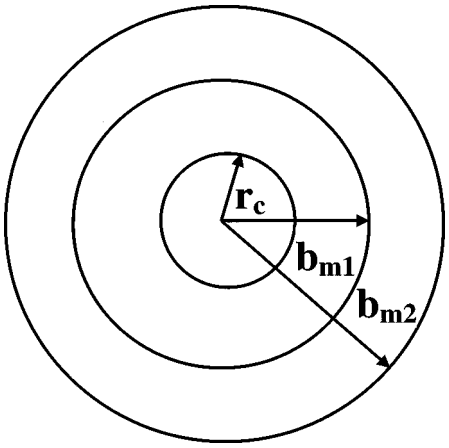

FIG. 1. A section of the collision sphere. r_c is the critical radius. All trajectories with impact parameter equal or smaller than r_c are defined as effective trajectories. b_{m1} and b_{m2} are impact parameters larger than r_c. Trajectories with impact parameter between r_c and b_{mi} are defined as ineffective and are not considered in the calculations of $P(E',E)$.

When a comparison with experimental results and previous calculations was required, the values of $\langle \Delta E \rangle$ obtained from the calculations were multiplied by the factor (b_m/b_{ref}).[2] b_{ref} is the product of σ_{LJ}, the Lennard-Jones collision radius, and $(\Omega^{2,2*})^{0.5}$, the collision integral. The value used in all the calculations is 0.520 nm.

B. Effective trajectories

It is hard to define a collisional event in classical trajectory calculations since some trajectories may occur at very large distances where no intermolecular interactions can possibly take place. Therefore, it is imperative that a criterion be established which separates elastic collisions which emanate from large impact parameter trajectories from collisions which couple the energetics of the bath and the molecule. The latter may or may not have a net energy exchange and thus are defined as elastic or inelastic depending on the outcome. Figure 1 shows a cross section of a collision sphere. The critical radius r_c indicates the radius of the sphere within which the energies of the bath and the molecule are coupled. b_{m1} and b_{m2} are two arbitrary b_m which are used in particular trajectory calculations. In a given sample of N trajectories with any arbitrary value of b_m, N_{eff} fall within the cross section defined by r_c. The ratio N_{eff}/N is given by the ratio $(r_c/b_m)^2$. N_{eff} is the important quantity because it, and not N, defines the value of $P(E',E)$. The value of r_c is not known and the present work suggests a way of evaluating N_{eff} from the outcome of the trajectory calculations. This will be based on the distance of closest approach, the least minimal distance-LMD, of the bath atom to the atoms in the colliding molecule.

C. Calculations of $P(E',E)$

The major objective of obtaining $P(E',E)$ is to use it in a master equation which enables the calculation of a reaction rate coefficient, k_{uni},

$$df(E,t)/dt = -[M]\int_0^\infty \{Z(E)P(E',E)f(E,t)dE - (Z(E')P(E,E')f(E',t)dE'\} - k(E,J), \tag{1}$$

$P(E',E)$ includes, of course, J and J', the initial and final rotational quantum numbers. $k(E,J)$ is the RRKM (Rice–Ramsperger–Kassel–Marcus) theory energy and J dependent rate coefficient and $f(E,t)$ is the energy and time dependent population of reacting molecules. $[M]$ is the bath concentration and $Z(E)$ is the collision number. (At not too high temperatures, the smallest absolute value of the eigenvalue of the master equation matrix is the rate coefficient,[1(b)] k_{uni}. At higher temperatures there is more than one eigenvalue which contribute to k_{uni} and the full matrix must be solved.[1(b)]) Finding the functional form of $P(E',E)$, therefore, is of great theoretical and practical importance in the investigations of chemical reactions.

The colliding molecules posses vibrational and rotational energies. The latter can be divided into two parts, active rotations, E_{ac}, which couple and exchange energy with the vibrational modes and overall adiabatic rotations, E_{ad} which do not exchange energy with the internal modes.[5(m),5(q),5(u)] Each type of rotational energy effects the unimolecular rate coefficient, $k(E,J)$, in a different way. The active rotations are included, with the vibrational energy, in the internal energy E while the inactive ones, those related to the angular momentum J, have centrifugal effects which affect the transition state. Theories such as RRKM and statistical adiabatic channel model (SACM) take explicit account of the contribution of the various energies to the unimolecular rate coefficient. These energies, obviously, also affect $P(E',E)$.

The energy transfer probability function is defined by the equation

$$P(E',E) = N(E',E)/N_{\mathrm{eff}}/\delta E. \tag{2}$$

$N(E',E)$ is the number of trajectories which transfer $\Delta E = E' - E$ and δE is the energy interval within which $N(E',E)$ is evaluated.

$P(E',E)$ must be normalized and must obey detailed balance. Normalization is automatically obtained from the definition of $P(E',E)$. However, detailed balance is a more complicated affair. In classical trajectories, time reversibility requires that for given initial and final conditions of a given trajectory the probabilities for forward and backward exchange of ΔE are equal. Those probabilities must be properly averaged over all impact parameters, orientations and allowed translational energies in the forward and backward directions to obtain the proper fluxes in both directions. These complications make an analytical expression (which can be used in checking for detailed balance) hard to come by. Given that the proper statistical averaging is done, to obtain detailed balance the initial energy dependence of $P(E',E)$ requires a matrix with a fine energy grid of $P(E',E)$. Such an undertaking will make a detailed study extremely expensive in time and resources. All these difficulties not withstanding, it will be shown that detailed balance is obtained over a very wide range of initial energies.

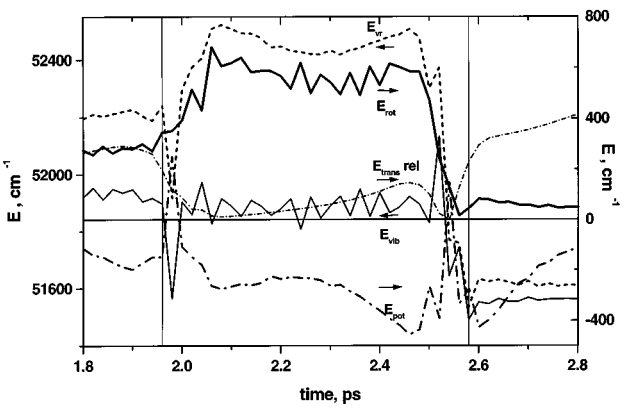

FIG. 2. The evolution of various system energies vs time during a trajectory. The two vertical lines indicate the beginning and the end of the collision. E_{vr} (— — —) is the vibrational rotational energy. E_{rot} (——) is the rotational energy. E_{trans} (—·—·) is the relative translational energy. E_{vib} (—) is the vibrational energy. E_{pot} (—·—) is the potential energy. Arrows indicate left or right ordinate.

III. RESULTS AND DISCUSSION

A. Intermolecular potentials

Collisional energy transfer is due to intermolecular interactions which are a function of the pairwise intermolecular potential. An example of the time evolution of the vibrational–rotational energy and the potential energy during a trajectory for a pairwise Lennard-Jones, L-J, potentials is given in Fig. 2. It changes during the trajectory lifetime in a dramatic way. Attention is drawn to the line representing the potential energy. The evolution of the potential energy during the lifetime of the trajectory shows a back to back L-J type behavior and a strong mixing with the internal modes during the collision. Thus, the coupling of rotation and internal modes affect the potential energy. The repulsive part peaks at the termination of the collision as determined by FOBS. This indicates the energy transferring ''kick'' at the end of the collision. It shows that regardless of the collision duration the actual energy transfer event takes place in a very short time during the end of the collision. This effect was discussed previously[5(r)] and will not be discussed here any further.

The multidimensional collision potential energy surface which is formed from the pairwise potentials is too complicated for practical use. Therefore in general applications, a pragmatic approach is used. An intermolecular potential, such as L-J is defined as a function of the center-of-mass, CM, distance. Gas collisions cross sections, for example, are all based on such pragmatic potentials. For ''pancake'' molecules like benzene, the distance of closest approach of the bath atom to one of the atoms in the molecule, minimal distance, MD, is more physically reasonable to use. The interactions in pancake molecules depend on the orientation of

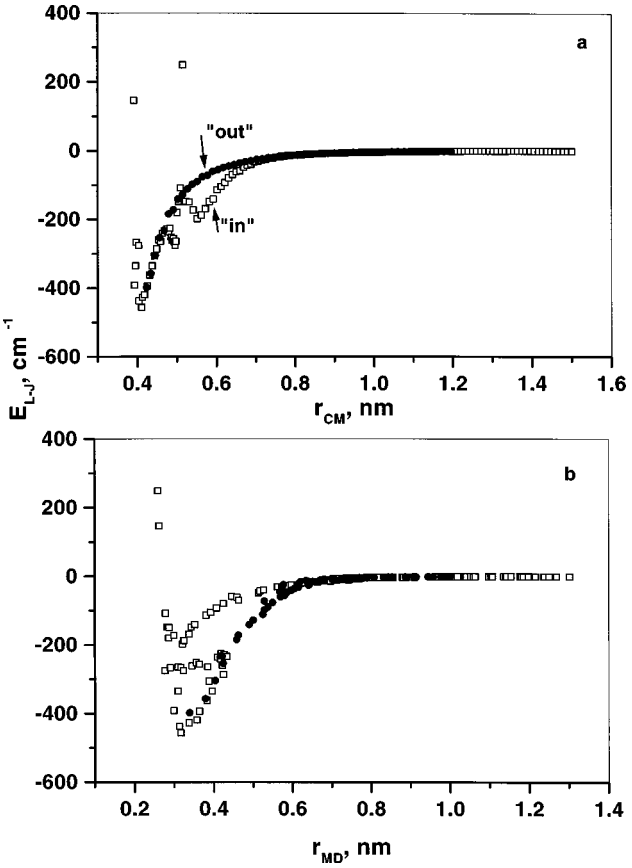

FIG. 3. The potential energy vs (a) the center-of-mass distance and (b) the minimal distance during the trajectory in Fig. 2 for Lennard-Jones pair-wise potential.

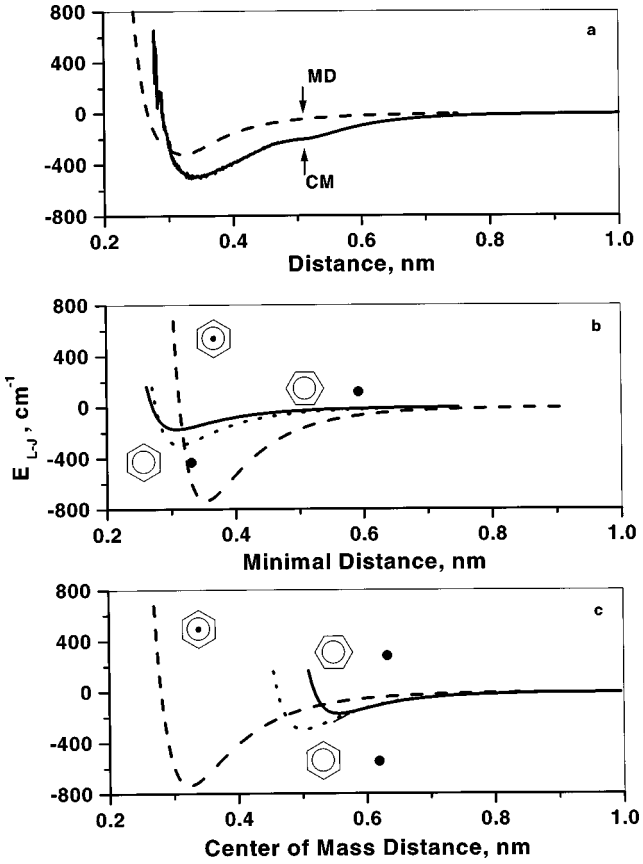

FIG. 4. The potential energy vs distance for pair-wise Lennard-Jones potential. (a) The global potential obtained by averaging 40 000 trajectories. MD indicates minimal distance and CM indicates center of mass distance. (b) The potential energy vs MD as a function of three orientations of the atom (dot) with respect to the molecule. ——atom collinear with H atom in the plane of the molecule. ···atom between two carbon atoms in the plane of the molecule. – – – atom above the center of mass perpendicular to the plane of the molecule. (c) The potential energy vs CM distance for the three orientations.

approach, whether it is in the molecular plane or perpendicular to it. Therefore a CM ''spherical'' potential is a major misrepresentation of the physics of the system in as much as it does not take in consideration the severe asymmetry of the molecular system. The MD on the other hand, is a more robust single parameter since it represents the distance which affects the potential most during the lifetime of the trajectory.

The potential as a function of the MD during the lifecycle of a single trajectory exhibits a complicated behavior, Fig. 3. The outgoing minimal distances as the atom departs (full points) *after the collision is over*, as defined by FOBS, are superimposed on the incoming MD's. By the above definition, the outgoing potential samples only the attractive part of the potential and no positive spikes will be seen. The well depth of the in-and-out potentials are not exactly equivalent due to changes in the orientation of the molecule during the collision. In addition, since the potential energy changes during the collision due to coupling with the internal modes, the line exhibits ''noise'' like chatter. The two positive points are the repulsive potential at the beginning and at the end of the trajectory. Besides single trajectory potentials, which are of little practical use, it is possible to calculate average, or global, potentials. They are instructive since they represent a quantity based on averaging tens of thousand of trajectories with all possible orientations which can be compared with average experimental quantities. Global potentials are obtained by binning the potential energy as a function of MD or CM distance for all the trajectories and dividing the sum in each bin by the number of trajectories. Fig. 4(a) shows the average global potentials for $\sim$40 000 trajectories with all possible molecular orientations. These potentials are based on L-J pairwise potentials. Similar global potentials were obtained from *ab initio* pairwise potentials (not shown here). The parameters of the potentials are given in the Appendix. Best fits to the *global* potentials were obtained by using an equation of the type:

$$V(r)=a\ \exp(-cr)+br^{-6}. \tag{3}$$

The values of the parameters are given in Table I. It is clear from Fig. 4 that the MD and CM potentials are different and the minimum of the MD curve appears, as expected, at a shorter distance. The MD is the quantity which best describes the intermolecular interaction. This is so because when measuring the potential as a function of MD all orientations of atom molecule are possible and the line in Fig. 4 is a true representation of the potential. Therefore, it is used in the next sections as part of the method to evaluate $P(E',E)$. It should be pointed out that the pairwise L-J potential used in the present calculations were estimated from global ''ex-

TABLE I. Fitting parameters of the Benzene–Ar global interaction potential[a] obtained from trajectory calculation.

Parameter	Lennard-Jones		Hobza	
	CM[b]	MD[c]	CM	MD
b, $nm^6 \times cm^{-1}$	-3.071 ± 0.061	-0.788 ± 0.004	-0.557 ± 0.056	-0.557 ± 0.008
$a*10^{-6}$, cm^{-1}	7.374 ± 0.261	9.871 ± 0.153	6.387 ± 0.419	3.793 ± 0.079
c, nm^1	25.03 ± 0.18	31.49 ± 0.08	25.10 ± 0.28	29.08 ± 0.13

[a] $V(r) = a \exp\{-cr\} + br^{-6}$.
[b] CM-Center-of-mass distance.
[c] MD-Minimal distance.

perimental'' L-J potentials by the method of Ref. 5(m). The fact that Eq. (3) (in MD coordinate) is a Buckingham-type potential and not the original L-J is an indication that the inversion of a global potential to pairwise is complicated and should consider all possible orientation plus molecular couplings at shorter distances.

The potential in CM coordinate, Fig. 4, was also fit by the use of Eq. (3). The parameters of the fit are given in Table 1. A more successful fit was obtained by adding a r^{-12} term to Eq. (3). The value of χ^2 dropped by a factor of 4, from 1380 to 340. This is no surprise since adding more parameters always ensures a better fit. (Adding an additional term to the MD expression did not change the value of χ^2 at all.) The potential in CM coordinate is not a smooth function. There is a plateau in the curve around 0.5 nm. The reason for the plateau is that many collisional orientations become excluded at short distances. This can be seen from Fig. 4(c). The minima in the potential curves for in plane collisions is at distances >0.5 nm. Any in-plane or near in-plane collision will not contribute to the potential at shorter distances. On the other hand, the MD curve does not suffer from such irregularities and MD it is therefore the parameter to use. Figures 4(b) and 4(c) show the asymmetry of the potential for three set configurations. The well depth is the deepest when the atom is centered above the ring and is the shallowest when the atom is in the plane of the molecule collinear with an H atom. In Fig. 4(c) if one subtracts the CM-carbon distance and the C–H distance from the distance of minima in the potential of the planar approach one sees that the minima for the wells for perpendicular and planar approaches lie at the same distance. That is to say, converting CM distances to MD brings the minima closer together as can indeed be seen in Fig. 4(b).

The position of the minima in the global potentials in the CM and MD coordinates are ~ 0.35 and ~ 0.32 nm, respectively. These values are close to the pairwise $\sigma_{\mathrm{C-Ar}} = 0.339$ nm and $\sigma_{\mathrm{H-Ar}} = 0.324$ nm but different from the effective $\sigma_{\mathrm{Benzene-Ar}} = 0.447$ nm and the collision integral corrected value of 0.520 nm. The discrepancy in the values underlies the problematic in converting effective potentials to pairwise potentials. Using the latter and averaging over all possible orientations to give a global potential does not yield back the starting effective potentials.

B. Effective trajectories

As indicated above, the key to obtaining reliable $P(E',E)$ is to sort the trajectories into effective and non-effective trajectories. The effective trajectories are those that fall inside the effective collision sphere and the ''non-effective'' are those outside the sphere that do not contribute to the energy transfer process because of negligible intermolecular interactions between the colliders. The first step in finding the number of the effective trajectories is to obtain the histograms of ΔE_{d} and ΔE_{up} vs the operational parameter which in our case is the lowest value the minimal distance obtains during a trajectory, the least minimal distance-LMD. The width of each bin in the histogram δ, is the smallest possible value such that the histogram can be replaced by a continuous function.

Sample histograms (only the end points are plotted) are shown in Fig. 5(a) for $b_m = 0.9$ and 1.5 nm at LMD intervals of $\delta = 1.0*10^{-3}$ nm. Each bin contains the percent accumulated values of ΔE. That is to say

$$\%\sum \Delta E = 100 \sum_i^n \Delta E_{ij} \Big/ \sum_j^m \sum_i^n \Delta E_{ij},$$

where n is the number of trajectories in bin j each transferring a quantity of energy ΔE_{ij}. m is the number of bins. As can be seen, there is complete overlap of the two lines of $\%\Sigma\Delta E$ vs the LMD. This is reasonable and expected since trajectories with the LMD outside the effective sphere (Fig. 1) do not contribute to the energy exchange and the values of $\langle \Delta E \rangle$ do not change when b_m is increased arbitrarily above the value of the critical impact parameter, r_c. There is a cut-off at 0.33 nm. Above this value almost no energy is transferred. The percent accumulated energy transferred is also shown on the right hand side of Fig. 5(a). At the cut-off the integral is 96%. The remaining 4% are contributed by the remaining 10 000 or 40 000 trajectories (see below) which are defined as ineffective. These trajectories also go undetected by FOBS and the 4% represents the accuracy of the calculations.

The same figure also shows the number of trajectories as a function of the LMD. The graph can be deconvoluted into two peaks. The sharp peak with a cut-off at 0.33 nm represents those trajectories which contribute to the energy transfer and the long tail can be assigned to elastic trajectories outside the collision sphere. For $b_m = 0.9$ nm, 10 000 out of 20 000 trajectories fall in the area of the sharp peak and are designated as effective trajectories. For $b_m = 1.5$ nm only 10 000 out of $\sim 50\,000$ trajectories form the sharp peak and are effective. It is expected, of course, that the percent of effective trajectories at 0.9 nm will be much larger than for

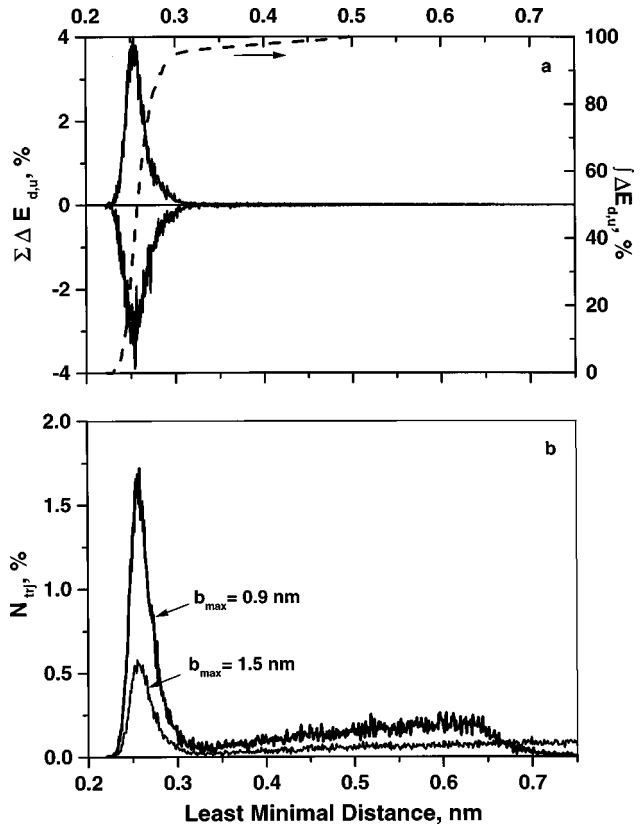

FIG. 5. (a) (Left ordinate) Percent ΔE transferred in collisions vs the distance of closest approach in a collision (minimal distance). (Right ordinate, dotted line, in the direction of the arrow) The integral of the figure of the left hand side vs the minimal distance. (b) Percent trajectories vs the minimal distance. The internal energy was 24 000 cm^{-1}. 20 000 and 50 000 cm^{-1} trajectories were run at impact parameters 0.9 and 1.5 nm, respectively. The total number of effective trajectories in both cases was 10 000.

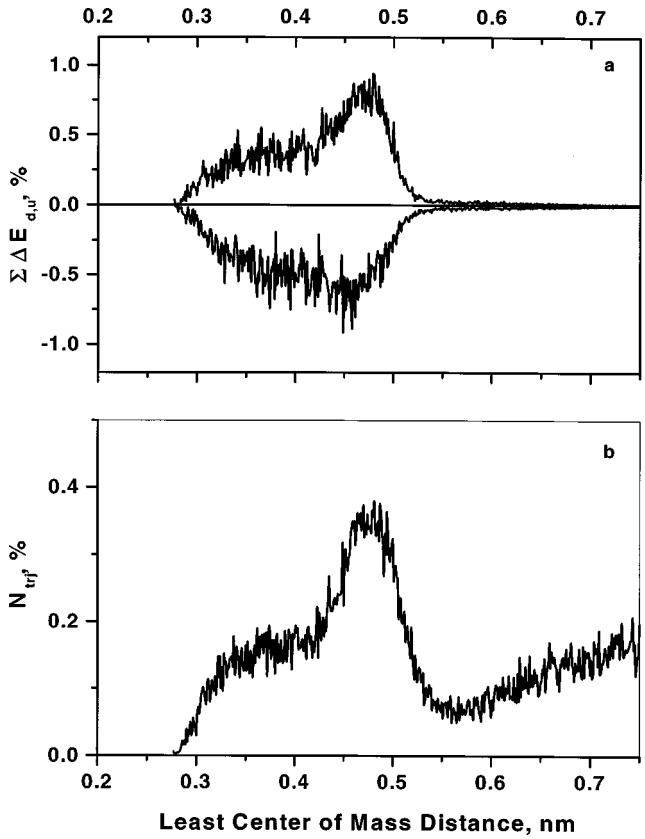

FIG. 6. (a) Percent ΔE transferred in collisions vs. the center of mass distance. (b) Percent trajectories vs the center-of-mass distance. The internal energy was 24 000 cm^{-1}. 20 000 and 50 000 cm^{-1} trajectories were run at impact parameters 0.9 and 1.5 nm, respectively. The total number of effective trajectories in both cases was 10 000.

1.5 nm because as the impact parameter increases the number of elastic collisions increases.

The value of r_c can be calculated from the relation: $r_c/b_{mi}=(N_{\text{eff}}/N_{\text{bmi}})^{0.5}$ where N_{eff} is the number of effective trajectories, b_{mi} is any maximum impact parameter and N_{bmi} is the total number of trajectories at the given b_{mi}. For $b_m=0.9$ nm and total number of trajectories of 20 000 the value of r_c can be calculated from: $(r_c/0.9)^2=10\,000/20\,000$ which yields $r_c=0.64$ nm. Using this value to estimate the total number of trajectories at $b_m=1.5$ nm that will yield 10 000 effective trajectories one obtains $(1.5/0.64)^2=N/10\,000$ and $N=55\,000$. This is close enough to the $\sim 50\,000$ trajectories found in the present calculations. b_m and r_c are measured from the center of the benzene ring to the center of the bath atom.

The tail of the curve in Fig. 5 for $b_m=0.9$ nm peaks around LMD of 0.62 nm and decays and reaches 0 at around 0.9 nm. The initial increase in the number of trajectories in the broad tail as a function of LMD comes about because of steric effects. As the value of LMD increases more orientations become available for energy exchange. Since the impact parameters is measured from the CM of the benzene molecule, at short LMD only perpendicular approaches are possible because the distances to the CM are the shortest. As the LMD increases other orientations become accessible and the number of trajectories increases. Above 0.62 nm again planar configurations become excluded since the peak must terminate at 0.90 nm which is the value of b_m. When the distance CM–C and C–H of 0.29 nm is added to the location of the peak at 0.62 nm the value of b_m is obtained. This means that planar configurations are excluded at LMD above 0.62 nm. This explains the fall-off to zero for larger values of LMD. The tail of the 1.5 nm curve is, as expected, much longer and extends beyond the limits of the figure up to LMD=1.5 nm.

When ΔE and N_{traj} are plotted vs the lowest value of the CM distance LCM, instead of the LMD the histograms are totally different, Fig. 6. There is no clear distinction between effective and elastic collisions but only smeared structureless lines. The reason for that is not difficult to understand. A trajectory with impact parameter 0 and line of approach in the plane of the molecule will have energy transfer occurring at LCM distances much larger than when the line of approach is perpendicular to the ring. Thus ΔE transfer can occur over a wide range of LCM distances unlike LMD which is a much more restrictive and limiting parameter and practically independent of molecular orientations.

The value of N_{eff} was checked by a different method. As can be recalled, the FOBS method defines the collision duration by sensing the first and last instances in which there is

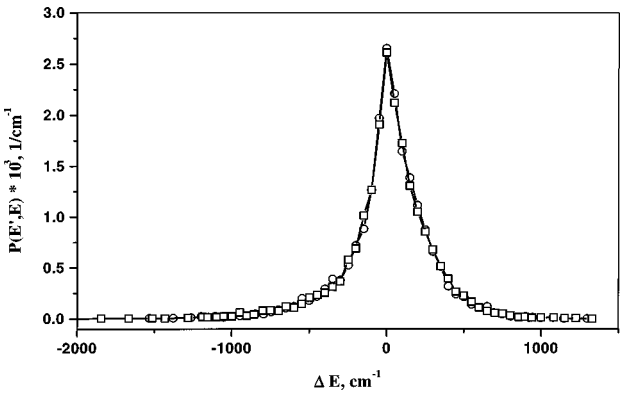

FIG. 7. $P(E',E)$ vs ΔE for impact parameters 0.9 nm □ and 1.5 nm ○. The internal energy is 37 500 cm^{-1}. The number of effective trajectories was 10 000.

a change ε in the internal energy. This method enables us, therefore, to distinguish between trajectories with finite collision duration and trajectories with zero duration (noncollisions). The latter have an internal energy change smaller than ε. The trajectories in the first category were defined as the effective trajectories and only those were used in the calculations of $P(E',E)$. The values of N_{eff} obtained by the FOBS method were within 5% agreement with the values obtained by the first method discussed above.

C. Calculations of $P(E',E)$

As discussed in the introduction, the source of uncertainty in the values of the energy transfer probability function emanates from the unknown value of $P(E,E)(\Delta E=0)$. Even though this value does not enter explicitly into the master equation it does affect the transition probability for values of ΔE different than 0. Thus, there is a need for an independent evaluation of $P(E,E)$ which originates from elastic collisions within the collision sphere. In the following we propose a method for finding $P(E',E)$ without making assumption about the unknown value of $P(E,E)$. The method is based on finding independently the value of N_{eff} which in turn is found by the LMD method and/or the FOBS method described above.

We calculate $P(E',E)$ by binning the effective trajectory in intervals of $\Delta E=50$ cm^{-1} bins and dividing the number of trajectories in each bin, $N(N',E)$, by N_{eff}. In creating the histograms a variable binning method is used. After the initial binning process is completed, the trajectories in each bin of width ΔE are averaged and the center of the bin is replaced by the average value of that bin. If the number of trajectories in a bin is less than a statistical sample, the width of the bin is increased in a systematic way until the proper sample is obtained. Figure 7 shows $P(E',E)$ for two impact parameters of 0.9 and 1.5 nm. $P(E',E)$ is independent of b_m and there is total overlap between the two lines. This is the expected result from the method proposed here. The total number of trajectories is 20 000 and 50 000 for 0.9 and 1.5 nm, respectively, and in both cases the number of effective number of collisions is 10 000.

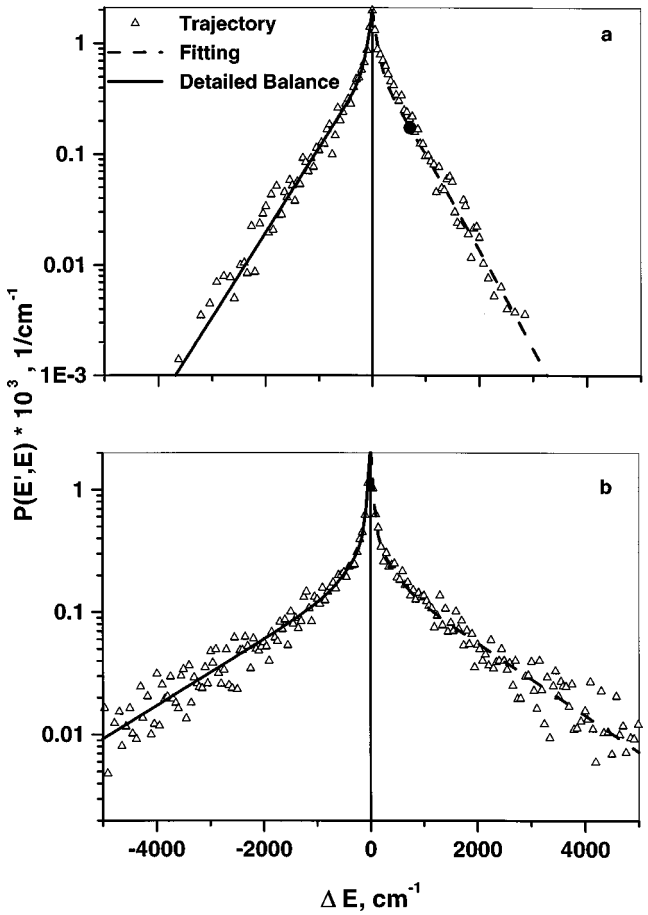

FIG. 8. $P(E',E)$ vs ΔE. The points are trajectory results. The full line is the fit to the data. The barred line is calculated by detailed balance. (a) Internal energy 6300 cm^{-1}. The full dot is the exact calculation of detailed balance (see text). (b) Internal energy 40 600 cm^{-1}. The impact parameter is 0.9 nm. 10 000 effective trajectories.

For $P(E',E)$ to be realistic it must obey detailed balance. It also must yield back, upon integration of the proper analytical expressions of $P(E',E)$, the values of $\langle\Delta E\rangle_{\text{d}}$, $\langle\Delta E\rangle_{\text{up}}$, and $\langle\Delta E\rangle_{\text{all}}$ obtained directly from trajectory calculations by the expression $\langle\Delta E\rangle_j=\Sigma\Delta E_{ij}/N_{\text{eff}}$. Note that averaging is done by dividing by N_{eff} and not by N_{total}. Figure 8 shows an example of $P(E',E)$ obtained directly from trajectory calculations by the present method, Eq. (2), a best fit to it, Eq. (4) and detailed balance (see discussion below)

$$P(E',E)_{\text{fit}}=\Sigma a_i \exp(-\Delta E/\alpha_i). \tag{4}$$

The various $\langle\Delta E\rangle$ quantities are then calculated by

$$\langle\Delta E\rangle_i=\int \Delta E_i P(E',E)_{\text{fit}}d\Delta E/\int P(E',E)_{\text{fit}}d\Delta E. \tag{5}$$

The limits of the integration depends on whether it is up, down or all.[1(b)] A comparison between the values of $\langle\Delta E\rangle_i$ obtained directly from trajectories and those obtained from Eq. (5) show that the agreement between the two values, in most cases, is better than 10% which is within the overall error of the calculations.

We now discuss the question of detailed balance, Eq. (6). Detailed balance is obtained in canonical systems where all the degrees of freedom are in thermal equilibrium defined

TABLE II. Fitting parameters for the best fit, Eq. 4, for Benzene–Ar collisions. $N_{\text{eff}}=10\,000$ trajectories, $b_m=0.9$ nm. All values of α are in cm^{-1}.

E_{vib}, cm^{-1}	T, K	Down	Up	Down	Up	Down	Up
6300	904	α_1		α_2			
		80 ± 5	50 ± 3	570 ± 31	450 ± 12		
		a_1*10^3		a_2*10^3			
		1.32 ± 0.05	0.98 ± 0.03	0.66 ± 0.04	1.03 ± 0.03		
7000	904	α_1		α_2			
		83 ± 5	50 ± 3	580 ± 37	440 ± 10		
		a_1*10^3		a_2*10^3			
		1.38 ± 0.05	1.01 ± 0.03	0.65 ± 0.05	1.05 ± 0.02		
24000	904	α_1		α_2		α_3	
		61 ± 5	44 ± 4	271 ± 115	441 ± 15	766 ± 163	⋯
		a_1*10^3		a_2*10^3		a_2*10^3	
		1.35 ± 0.1	1.17 ± 0.04	0.50 ± 0.1	1.02 ± 0.04	0.35 ± 0.2	⋯
24000	1950	α_1		α_2		α_3	
		70 ± 2	60 ± 3	550 ± 211	310 ± 130	1480 ± 453	1020 ± 108
		a_1*10^3		a_2*10^3		a_3*10^3	
		1.52 ± 0.04	1.35 ± 0.06	0.28 ± 0.01	0.24 ± 0.05	0.18 ± 0.01	0.33 ± 0.07
40570	2812	α_1		α_2		α_3	
		40 ± 2	50 ± 2	270 ± 56	350 ± 50	1600 ± 134	1540 ± 147
		a_1*10^3		a_2*10^3		a_3*10^3	
		1.82 ± 0.05	1.77 ± 0.03	0.31 ± 0.04	0.29 ± 0.04	0.21 ± 0.02	0.20 ± 0.02

by a temperature. We have, therefore, performed trajectory calculations for thermal systems. The internal energy of the molecule was chosen, its vibrational temperature determined[10] and the rotational and translational energies were chosen randomly from the appropriate Boltzmann distributions at that temperature. $P(E',E)$ is a function of the internal vibrational–rotational energy, E. Therefore, when verifying the detailed balance expression

$$f(E)P(E',E)=f(E')P(E,E'), \tag{6}$$

the probability must be known at all initial energies. This is a formidable task and a lifetime occupation. There are shortcuts which can be taken. The dependence of $P(E',E)$ on E can be expressed in an empirical parametric expression.[6(a)] This is not good enough for an exact study which explores the basic principles of the method. We have therefore done very detailed studies at two energy ranges. In a high energy range where $P(E',E)$ is not expected to be a function of the energy ($\langle\Delta E\rangle$ was found experimentally to be independent of $E^{2(g)}$) and in a low energy range where we could check only a limited number of points for detailed balance.

In the high energy range we have checked $P(E',E)$ for detailed balance at 5 temperatures. We report the results for one. Figure 8(b) shows $P(E',E)$ for benzene with initial internal energy of 40 570 cm^{-1} which is equivalent to ensemble temperatures of 2812 K. The dots represent the trajectory results. Each dot represents the average ΔE in each bin as discussed above. The line on the down collision side is a best fit to the trajectory data points. This line was used in Eq. (6) to obtain the up-collision part of $P(E',E)$ which is represented by the broken line on the up-wing side of the curve. The agreement is perfect. Considering that in no stage in the calculations, detailed balance was introduced explicitly or implicitly, the results attest to the robustness of the procedure of obtaining $P(E',E)$. The logarithmic representation of $P(E',E)$, shows that the fit and detailed balance are good over many orders of magnitude. This fit to the down collision side was obtained, in this energy range, by using a triexponential function, Eq. (6). The values of the coefficients of the fitting function are given in Table II.

The values of α_1 and α_2 can both be ascribed to weak collisions and only α_3 represents the strong collision part. The values of the fitting parameters indicate that $\sim 9\%$ of the all collisions are described by the high energy part of the $P(E',E)$ function. This does not mean, of course, that $\sim 9\%$ of the collisions are supercollisions.[11] Actually, there is only a very small number of supercollisions at the high energy tail of the distribution.[6(b)] Most of the collisions described by the high energy part contribute low ΔE values to the total amount of energy transferred.

For the low energy range we have studied a benzene molecule with internal energy of 6300 cm^{-1} (904 K) and 7000 cm^{-1}. Figure 8(a) shows the trajectory data. The full line is the best fit to the down collisions, Eq. (4), and the barred line is obtained from detailed balance, Eq. (6). The detailed balance line is good but the fit to the data is not as good as in the high energy cases. This is understandable since $P(E',E)$ is energy dependent in the low energy range. The full point is where exact detailed balance was performed and $P(E',E)$ at 7000 cm^{-1} was used. The agreement is good. The functional form of $P(E',E)$ in this range is biexponential. (At low energies the high ΔE's tail is absent). The parameters are given in Table II. The values of the weak collisions parts of $P(E',E)$ do not change with temperature (energy) while the strong collision parts do change in a very significant way. This indicates that temperature does affect mainly the large ΔE's while the small ΔE's are not effected by it.

As a check on the method, $P(E',E)$ was calculated by the FOBS method as described in the section dealing with N_{eff}. The curves calculated by the two methods (not shown)

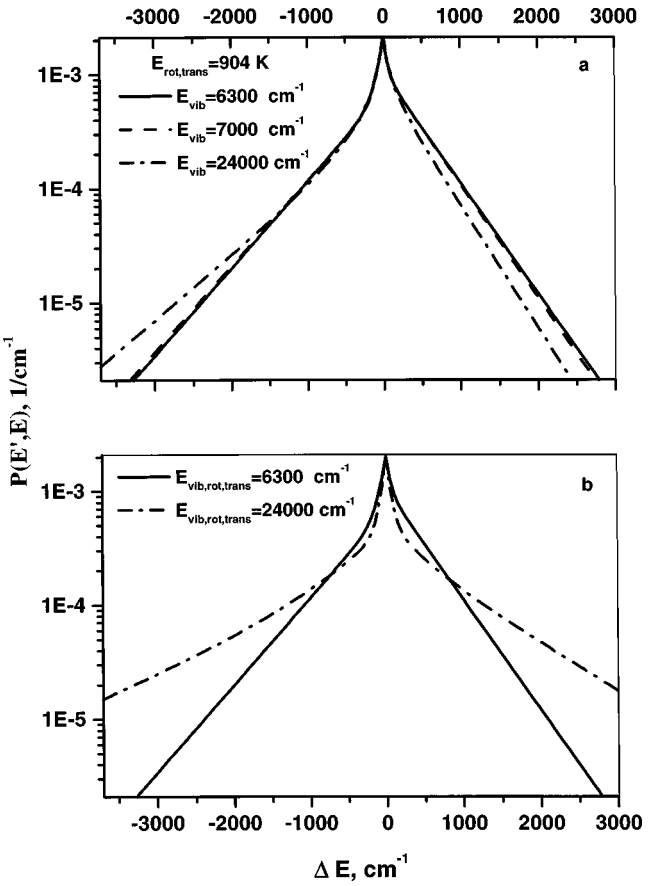

FIG. 9. $P(E',E)$ vs ΔE for thermal systems. $E_{vib}=6300\ cm^{-1}$ (——), 7000 cm^{-1} (— — —), 24 000 cm^{-1} (—·—·—). (a) $E_{vib}=6300\ cm^{-1}$ ($T=904$ K). (b) $E_{vib}=6300\ cm^{-1}$ ($T=904$ K) and 24 000 cm^{-1} (1950 K). 10 000 effective trajectories.

were identical for all practical purposes and could not be distinguished from each other.

D. The effect of internal energy and temperature on $P(E',E)$ and on $\langle\Delta E\rangle$

It is interesting to observe the evolution of $P(E',E)$ with internal energy E. Figure 9(a) shows 3 lines calculated at 904 K and internal energies of 6300 cm^{-1}, 7000 cm^{-1}, and 24 000 cm^{-1}. 904 K is the vibrational temperature of the benzene molecule at 6300 cm^{-1}. As expected the higher the internal energy the higher the asymmetry of the function. At 6300 cm^{-1} the system is at thermal equilibrium and up and down collisions are almost (but not exactly, due to detailed balance) equally probable. At higher energies the system will tend to equilibrium and down collisions prevail. The higher and farther the internal energy from the average thermal energy (6300 cm^{-1}) the larger the contribution of down collisions. It is interesting to compare the two $P(E',E)$ functions at two energies each at its own thermal equilibrium, Fig. 9(b). The same arguments used in discussing the 6300 cm^{-1} line in Fig. 9(a) can be used here. The lines are almost symmetrical because the internal energy is also the canonical average thermal energy. The $P(E',E)$ functions are totally different from one another. The high energy curve is much broader which indicates the prevalence of high ΔE's. This explains the results given in Table II. At low temperatures where there are no high ΔE's a biexponential function is the best fitting function. At high temperatures triexponential functions are needed to fit the data. The third exponential takes care of the high energy wings of $P(E',E)$. When a molecule with high internal energy 24 000 cm^{-1} is put in a cold bath (average thermal energy of 6300 cm^{-1}) the down wing is very broad and a triexponential function is needed to fit the data. The up collisions wing, on the other hand, is much narrower (up collisions will carry the system away from equilibrium) and a biexponential function is the best fit to the data, Table II.

TABLE III. Various $\langle\Delta E\rangle$ quantities for Benzene–Ar collisions in thermal systems. 20 000 trajectories, $b_m=0.9$ nm. All energies in cm^{-1}.

E_{vib}	T, K	$\langle\Delta E\rangle_{all}$[a]	$\langle\Delta E\rangle_d$	$\langle\Delta E\rangle_{up}$
		$\langle\Delta E_{tot}\rangle$		
6300	904	−11	−477	421
24000	1950	−62	−881	775
		$\langle\Delta E_{vib}\rangle$		
6300	904	95	−115	235
24 000	1950	171	−320	555
		$\langle\Delta E_{rot}\rangle$		
6300	904	−106	−552	366
24 000	1950	−233	−1107	664

[a] $\langle\Delta E\rangle=\Sigma(\Delta E_i)/N_{eff(total,d,u)}$.

The overall average energy transferred per collision, $\langle\Delta E\rangle_{all}$ and the average energy transferred in up, $\langle\Delta E\rangle_{up}$, and down, $\langle\Delta E\rangle_d$, collisions were calculated for two thermal systems with average energies of 6300 cm^{-1} and 24 000 cm^{-1}, Table III. The higher the temperature the higher the absolute value of $\langle\Delta E\rangle_i$ (i indicates up, down, and all). The values of $\langle\Delta E\rangle_i$ increase with temperature. There is no experimental thermal data for energy transfer between benzene and Ar. However, the value of $\langle\Delta E\rangle_d$ is in accord with similar polyatomic systems colliding with Ar.[1(a)] Table III also gives the values of $\langle\Delta E_{vib}\rangle$ and $\langle\Delta E_{rot}\rangle$. It shows that, for thermal systems, up collisions prevail in internal energy transfer and down collisions prevail in rotational energy transfer. As the molecule moves from the equilibrium average energy after the first collision the trend will reverse and down collisions will dominate. It should be pointed out again that $\langle\Delta E\rangle_i$ is calculated by using N_{eff} and not the total number of trajectories. Therefore, all values of $\langle\Delta E\rangle_i$ reported in this work are higher than those found in previous trajectory calculations which use N_{total} as the normalizing and averaging factor.

E. The effect of rotations on $\langle\Delta E\rangle$

In a previous study[12] it was found that rotations play a major role in collisional energy transfer. It was found that ''freezing'' out the rotations has a major effect on the value of $\langle\Delta E\rangle$. Even for highly vibrationally excited molecules, where normally down collisions are dominant, up collisions prevail as T-R energy transfer causes $\langle\Delta E\rangle$ to increase. The question which remained is the dependence of $\langle\Delta E\rangle$ on the rotational temperature. To study that, the molecule with in-

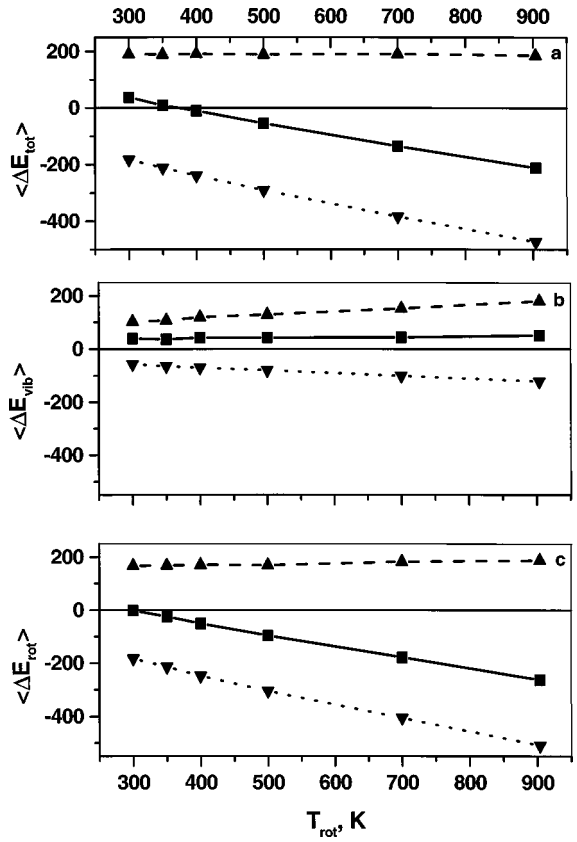

FIG. 10. The rotational, vibrational, and total average energies transferred in up ▲, down ▼, and all ■ collisions. The internal energy is 6300 cm^{-1} and the translational energy is 300 K.

ternal energy of 6300 cm^{-1} ($T=904$ K) was allowed to collide with an Ar atom at 300 K. The rotational temperature of the molecule was varied from 300 K to 904 K. It was found that the changes in the rotational temperature have a major impact on the values of $\langle \Delta E \rangle$. Figure 10 shows that $\langle \Delta E \rangle_{\rm all}$ and $\langle \Delta E_{\rm rot} \rangle$ change dramatically with $T_{\rm rot}$ while $\langle \Delta E_{\rm vib} \rangle$ is almost constant. This is misleading in a way, since the up and down values of $\langle \Delta E_{\rm vib} \rangle$ do change in a significant way. On the other hand, while the values of the down collisions of $\langle \Delta E_{\rm rot} \rangle$ change significantly the up values remain constant. Where does it all lead us? It indicates that the values of $\langle \Delta E \rangle_{\rm all}$ do not represent the true processes which take place during collisions and it is the up and down values which better describe the physics of the energy transfer process.

The values of $\langle \Delta E \rangle_{\rm all}$ as well as those of $\langle \Delta E_{\rm vib} \rangle$ and $\langle \Delta E_{\rm rot} \rangle$ are very sensitive to $T_{\rm rot}$ [as found also in Ref. 5(p)]. A slight heating of the rotations during one collision will cause a significant change in the value of $\langle \Delta E \rangle$ in a subsequent collision. This consideration is important in nonthermal systems where the initial rotational temperature might be ambient temperature but there is no guarantee that rotational heating does not take place during the relaxation process. To check this point we have calculated $\langle \Delta E \rangle_{\rm all}$ by running 5000 trajectories at internal energy of 24 000 cm^{-1} and rotational temperature of 350 K. The value of $\langle \Delta E \rangle_{\rm all}$ changed from 19 cm^{-1} to -5 cm^{-1}. To compare with experimental results this value must be multiplied by $(r_c/b_{\rm ref})^2$. The value of r_c from the present calculations is 0.64 nm and the value of $b_{\rm ref}$ from Barker's work[2(b)] is 0.354 nm. Therefore, the corrected value of $\langle \Delta E \rangle_{\rm all}$(exp) is -16 cm^{-1}, not too far from the reported experimental value of[2(b)] -30 cm^{-1}. Considering the complicated inversion procedures of the experimental data[2(b)] on one hand and the inversion of global potentials to pairwise potentials used in trajectory calculations on the other hand, the agreement is more than satisfactory. This has important ramifications on the way trajectory calculations are compared with experimental data. Currently, when a comparison is made between the values of $\langle \Delta E \rangle$ obtained by trajectory calculations with those obtained by experiments, the zero point energy of the molecule is added to the value of the experimental excitation energy. This way, a reasonable agreement is obtained between experiments and calculations. This is a somewhat arbitrary procedure since there is no zero point energy associated with classical calculations. However, if rotational heating is considered as part of the energy transfer process, agreement can probably be obtained with experiment without invoking zero point energy.

IV. CONCLUSIONS

A novel method to calculate collisional energy transfer probability density function, $P(E',E)$, from quasi-classical trajectory calculations is proposed. The method eliminates the ambiguities in previous methods associated with the normalization procedure. It was found that $P(E',E)$ found by the proposed method obeys exactly conservation of probability and detailed balance. The principles of the method are:

(a) The average energy transferred is binned against the shortest distance of approach of the bath atom to the nearest atom to it in the molecule during the collision (least minimal distance, LMD). The least minimal distance above which no energy is transferred is noted.
(b) The number of trajectories is binned against the least minimal distance. All the trajectories that fall below the least minimal distance are designated as effective trajectories, $N_{\rm eff}$.
(c) $P(E',E)$ is calculated by dividing the number of trajectories which transfer ΔE between E and E' by the number of effective trajectories and by the energy interval in which the trajectories are binned, δE.

It was found that at low energies (vibrational temperatures) $P(E',E)$ can be represented by biexponential functions. At high energies triexponential functions are needed to obtain a best fit over four orders of magnitude. The reason for the added exponential at high energies is that $P(E',E)$ is much broader (large ΔE's are probable). The high ΔE tails are represented by the third exponential. The effects of temperature on $P(E',E)$ and on the average energy transferred per collision, $\langle \Delta E \rangle$, are reported as are the effects of the rotational temperature on the values of the latter. It is shown that rotational heating is part of the energy transfer mechanism and when taken in consideration, good agreement with experimental results is obtained without adding artificially zero point energy to the value of the internal energy.

Starting from pairwise *ab initio* or Lennard-Jones potentials, global potentials in center of mass or least minimal distance coordinates are calculated. The global potentials in the least minimal distance coordinate fit Buckingham type potentials. The global potential in center-of-mass coordinate can not be fit by a simple function because the intermolecular forces are strongly asymmetric in pancake-like benzene molecule.

ACKNOWLEDGMENTS

This work is supported by the Fund for the Promotion of Research at the Technion to (IO) and by the Ministry of Science and the Arts.

APPENDIX: INTERMOLECULAR POTENTIAL PARAMETERS

The Appendix includes all the parameters used in the calculations of the Lennard-Jones and *ab initio* intermolecular potentials.

1. Parameters for Lennard-Jones potential[5(o),5(p)]

$\sigma_{C-Ar}=0.339$ nm, $\sigma_{H-Ar}=0.324$ nm, $\varepsilon_{C-Ar}/k_B=48.2$ K, $\varepsilon_{H-Ar}/k_B=27.2$ K;

$\sigma_{eff}=0.447$ nm, $\varepsilon_{eff}/k_B=213$ K.

The pair-wise Lennard-Jones potential is given by the equation

$$V_{ij}=A_{ij}r_{ij}^{-12}-B_{ij}r_{ij}^{-6}; \quad i,j=1-6$$

where $A_{H-Ar}=78\,688\,303*10^{-12}$ cm^{-1} nm^{12}, $B_{H-Ar}=114\,035*10^{-6}$ cm^{-1} nm^{6}; and $A_{C-Ar}=416\,190\,471*10^{-12}$ cm^{-1} nm^{12}, $B_{C-Ar}=412\,411*10^{-6}$ cm^{-1} nm^{6}.

2. Parameters for ab initio potential[8(b)]

$\sigma_{eff}=0.453$ nm, $\varepsilon_{eff}/k_B=111$ K.

The *ab initio* potential is given by the equations

$$V=V^{REP}+V^{DISP};$$

$$V^{REP}=a_1\left\{\sum_{i=1}^{6}(C_1/r_{(H-Ar)i})^N+\sum_{i=1}^{6}(C_2/r_{(C-Ar)i})^N\right\};$$

$$V^{DISP}=a_2C_3\left\{-a_3\sum_{i=1}^{6}(1/r_{(H-Ar)i})^M(1-C_4/r_{(H-Ar)i})-a_4\sum_{i=1}^{6}(1/r_{(C-Ar)i})^M\right\},$$

where REP indicates the repulsive part of the potential and DISP indicates the dispersion part. The parameters used are:

$C_1=0.2808$ nm, $C_2=0.3685$ nm,

$C_3=0.361*10^{-6}$ nm^6/cm^{-1}, $C_4=0.271$ nm;

$N=13.31$, $M=6.0$;

$a_1=83.5936$ cm^{-1}, $a_2=8065.714$ cm^{-1},

$a_3=41.354\,96$ cm^{-1}, $a_4=118.2612$ cm^{-1}.

[1] (a) D. C. Tardy and B. S. Rabinovitch, Chem. Rev. **77**, 369 (1977); (b) I. Oref and D. C. Tardy, *ibid.* **90**, 1407 (1990).

[2] (a) Chapters, in *Vibrational Energy Transfer Involving Large and Small Molecules*, edited by J. R. Barker (JAI, Greenwich, Connecticut, 1995); (b) J. R. Barker and B. M. Toselli, Int. Rev. Phys. Chem. **12**, 305 (1993); (c) K. Luther and K. Reihs, Ber. Bunsenges. Phys. Chem. **92**, 442 (1988); (d) H. Hippler and J. Troe, in *Bimolecular Collisions*, edited by J. E. Baggott and M. N. Ashfold (The Royal Soc. of Chemistry, London, 1989); (e) A. S. Mullin, J. Park, J. Z. Chou, G. W. Flynn, and R. E. Weston, J. Chem. Phys. **53**, 175 (1993); (f) A. S. Mullin, C. A. Michaels, and G. W. Flynn, *ibid.* **102**, 6032 (1995); (g) M. Damm, H. Hippler, and J. Troe, *ibid.* **88**, 3564 (1988).

[3] (a) P. J. Robinson and K. A. Holbrook, in *Unimolecular Reactions* (Wiley-Interscience, New York, New York, 1972); (b) R. G. Gilbert and S. C. Smith, *Theory of Unimolecular and Recombination Reactions* (Blackwell Scientific Publications, Oxford, 1990).

[4] (a) K. F. Lim and R. G. Gilbert, J. Phys. Chem. **84**, 6129 (1986); **92**, 1819 (1990); (b) R. G. Gilbert and I. Oref, *ibid.* **95**, 5007 (1991); (c) E. I. Dashevskaya, E. E. Nikitin, and I. Oref, *ibid.* **97**, 9397 (1993); (d) **99**, 10797 (1995); (e) D. C. Tardy, J. Chem. Phys. **99**, 963 (1993); (f) D. C. Tardy and B. H. Song, J. Phys. Chem. **97**, 5628 (1993); (g) L. Ming, T. D. Sewell, and S. Nordholm, Chem. Phys. **83**, 199 (1995); (h) L. E. B. Borjesson and S. Nordholm, Chem. Phys. **112**, 393 (1996).

[5] (a) N. Date, W. L. Hase, and R. G. Gilbert, J. Phys. Chem. **88**, 5135 (1984); (b) N. J. Brown and J. A. Miller, J. Chem. Phys. **80**, 5568 (1984); (c) M. Bruehl and G. C. Schatz, *ibid.* **89**, 770 (1988); (d) J. Phys. Chem. **92**, 7223 (1988); (e) G. Lendvay and G. C. Schatz, *ibid.* **94**, 8864 (1990); (f) D. L. Clarke, E. G. Thompson, and R. G. Gilbert, Chem. Phys. Lett. **182**, 357 (1991); (g) G. Lendvay and G. C. Schatz, J. Phys. Chem. **96**, 3752 (1992); (h) D. L. Clarke, I. Oref, R. G. Gilbert, and K. F. Lim, J. Chem. Phys. **96**, 5983 (1992); (i) G. Lendvay and G. C. Schatz, *ibid.* **96**, 4356 (1992); (j) V. Bernshtein and I. Oref, J. Phys. Chem. **97**, 12811 (1993); (k) G. Lendvay and G. C. Schatz, J. Chem. Phys. **98**, 1034 (1993); (l) V. Bernshtein and I. Oref, J. Phys. Chem. **98**, 3782 (1994); (m) K. F. Lim, J. Chem. Phys. **100**, 7385 (1994); **101**, 8756 (1994); (n) V. Bernshtein, K. F. Lim, and I. Oref, J. Phys. Chem. **99**, 4531 (1995); (o) V. Bernshtein and I. Oref, Chem. Phys. Lett. **233**, 173 (1994); (p) T. Lenzer, K. Luther, J. Troe, R. G. Gilbert, and K. F. Lim, J. Chem. Phys. **103**, 626 (1995); (q) I. Koifman, E. I. Dashevskaya, E. E. Nikitin, and J. Troe, J. Phys. Chem. **99**, 15348 (1995); (r) D. C. Clary, R. G. Gilbert, V. Bernshtein, and I. Oref, Faraday Discuss. Chem. Soc. **102**, 423 (1995); (s) V. Bernshtein and I. Oref, J. Chem. Phys. **104**, 1958 (1996); (t) G. Lendvay and G. C. Schatz, J. Phys. Chem. **98**, 6530 (1994); (u) I. Rosenblum, E. I. Dashevskaya, E. E. Nikitin, and I. Oref, Mol. Eng. Mol. Eng. **7**, 169 (1997).

[6] (a) V. Bernshtein, I. Oref, and G. Lendvay, J. Phys. Chem. **100**, 9738 (1996); (b) **101**, 2445 (1997); (c) E. Tzidoni and I. Oref, Chem. Phys. **84**, 403 (1984).

[7] G. C. Schatz and G. Lendvay (private communication).

[8] (a) VENUS, Quantum Chemistry Program Exchange by W. L. Hase, R. J. Duchovic, X.Hu, K. F. Lim, D. H. Lu, G. Pesherbe, K. N. Swamy, S. R. Vande-Linde, and R. J. Rolf, Quantum Chemistry Program. Exchange Bull; (b) O. Bludsky, V. Spirko, V. Hrouda, and P. Hobza, Chem. Phys. Lett. **196**, 410 (1992).

[9] J. A. Draeger, Spectrochim. Acta A **41**, 607 (1985).

[10] J. Park, R. Bersohn, and I. Oref, J. Chem. Phys. **94**, 5700 (1990).

[11] (a) I. Oref, ''Supercollisions'' in *Vibrational Energy Transfer Involving Small and Large Molecules Vol. 2 of Advances in Chemical Kinetics and Dynamics*, edited by J. R. Barker (JAI, Greenwich, Connecticut, 1995); (b) A. Pashutzki and I. Oref, J. Phys. Chem. **92**, 1978 (1988); (c) S. Hassoon, I. Oref, and C. Steel, J. Chem. Phys. **89**, 1743 (1988); (d) I. M. Morgulis, S. S. Sapers, C. Steel, and I. Oref, *ibid.* **90**, 923 (1989); (e) L. A. Miller, C. D. Cooks, and J. D. Barker, *ibid.* **105**, 3012 (1996).

[12] (a) V. Bernshtein and I. Oref, J. Chem. Phys. **106**, 7080 (1997); (b) V. Bernshtein and I. Oref, ACS Symposium Series (in press).